J|A|C|S ARTICLES

Published on Web 07/07/2010

Design, Synthesis, and Study of Main Chain Poly(N-Heterocyclic Carbene) Complexes: Applications in Electrochromic Devices

Adam B. Powell, Christopher W. Bielawski, and Alan H. Cowley*

Department of Chemistry and Biochemistry and Center for Nano and Molecular Science and Technology, The University of Texas at Austin, 1 University Station, A5300, Austin, Texas 78712-0165

Received May 12, 2010; E-mail: cowley@mail.utexas.edu

Abstract: A series of poly(N-heterocyclic carbene) complexes in which the carbene functionalities are orthogonally connected to the main chains of the respective polymers have been synthesized via oxidative electropolymerization of various bis(bithiophene)-substituted monomers with appended transition metal or main group entities (M = Ir, Au, Ag, or S). The polymers were characterized using a range of electrochemical, X-ray photoelectron spectroscopy, UV−vis spectroscopy, profilometry, and four-point probe conductivity measurements. Most of the polymers exhibited an intense absorbance wave at 700 nm under oxidative conditions which was attributable to the formation of polarons along the main chains. The iridium-containing thin film poly(**8**) was found to possess a significant NIR absorbance at 1100 nm in which the metal moiety effectively functioned as an electron sink. Electrochemical analyses of the polymer thin films revealed that they exhibited highly reversible electrochromic phenomena.

Introduction

Electroconducting polymers (ECPs) have become an increasingly active area of research following the work of Shirakawa and co-workers in 1977 on the conducting properties of polyacetylene.[1] Organic ECPs, in particular, have been studied extensively and have found utility in many photovoltaic,[2] sensing,[3] and medicinal applications,[4] among others. Such materials are generally polymerized electrochemically since this methodology offers a number of advantages which include synthetic ease and the ability to deposit the polymer directly onto an electrode or conducting substrate of choice.[5] Thiophene is commonly used as a monomer for accessing ECPs due to its high functional group tolerance; however, ethylenedioxythiophene (EDOT) and bithiophene-based monomers are also often employed because they can be electrochemically polymerized at relatively low potentials.[6]

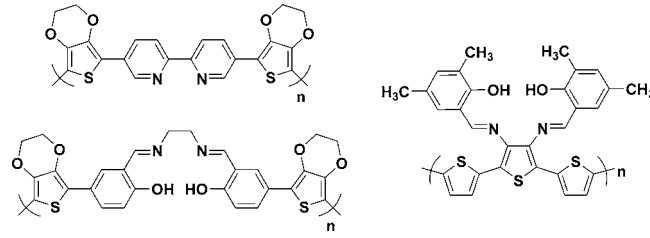

Figure 1. Examples of polymers synthesized via electropolymerization.

The incorporation of transition metal and main group atoms into ECPs has been shown to afford significant increases in conductivity, thus greatly expanding the utilities of these materials.[7] For example, the polymers shown in Figure 1 have been used for the support of elements which span the periodic table.[8] Of the various electropolymerizable scaffolds depicted, the most widely employed are those derived from the *N*,*N*′-ethylenebis(salicylimine) (Salen) ligand framework, mainly because such ligands can be prepared via simple condensation of ethylene diamine and salicylaldehyde. However, a notable

(1) Chiang, C. K.; Fincher, C. R.; Park, Y. W.; Heeger, A. J.; Shirakawa, H.; Louis, E. J.; Gau, S. C.; MacDiarmid, A. G. *Phys. Rev. Lett.* **1977**, *39*, 1098–1101.

(2) (a) Wong, W. Y.; Wang, X. Z.; He, Z.; Djurisic, A. B.; Yip, C. T.; Cheung, K. Y.; Wang, H.; Mak, C. S. K.; Chan, W. K. *Nat. Mater.* **2007**, *6*, 521–527. (b) Knapton, D.; Rowan, S. J.; Weder, C. *Macromolecules* **2006**, *39*, 651–657. (c) Hou, J. H.; Huo, L. J.; He, C.; Yang, C. H.; Li, Y. F. *Macromolecules* **2006**, *39*, 594–603. (d) Zhou, E.; Zhan'ao, T.; Lijun, H.; Youjun, H.; Chunhe, Y.; Yongfang, L. *J. Phys. Chem. B* **2006**, *110*, 26062–26067.

(3) (a) Wong, W. Y. *Dalton Trans.* **2007**, 4495–4510. (b) Holliday, B. J.; Stanford, T. B.; Swager, T. M. *Chem. Mater.* **2006**, *18*, 5649–5651. (c) Tennyson, A. G.; Do, L.; Smith, R. C.; Lippard, S. J. *Polyhedron* **2007**, *26*, 4625–4630. (d) He, S.; Iacono, S. T.; Budy, S. M.; Dennis, A. E.; Smith, D. W.; Smith, R. C. *J. Mater. Chem.* **2008**, *18*, 1970–1976.

(4) (a) Boopathi, M.; Won, M. S.; Shim, Y. B. *Anal. Chim. Acta* **2004**, *512*, 191–197. (b) Halldorsson, J. A.; Little, S. J.; Diamond, D.; Spinks, G.; Wallace, G. *Langmuir* **2009**, *25* (18), 11137–11141. (c) Moulton, S. E.; Imisides, M. D.; Shepherd, R. L.; Wallace, G. G. *J. Mater. Chem.* **2008**, *18* (30), 3608–3613. (d) George, P. M.; LaVan, D. A.; Burdick, J. A.; Chen, C. Y.; Liang, E.; Langer, R. *Adv. Mater.* **2006**, *18* (5), 577–581.

(5) Moorlag, C.; Clot, O.; Zhu, Y.; Wolf, M. O. *Macromol. Symp.* **2004**, *209*, 133–139.

(6) (a) Chen, X. Y.; Yang, X.; Holliday, B. J. *J. Am. Chem. Soc.* **2008**, *130*, 1546–1547. (b) Hesterberg, T. W.; Yang, X.; Holliday, B. J. *Polyhedron* **2010**, *29*, 110–115.

(7) (a) Kingsborough, R. P.; Swager, T. M. *J. Am. Chem. Soc.* **1999**, *121*, 8825–8834. (b) Kurashina, M.; Murata, M.; Watanabe, T.; Nishihara, H. *J. Am. Chem. Soc.* **2003**, *125*, 12420–12421.

(8) For recent reviews see: (a) Eloi, J. C.; Chabanne, L.; Whittel, G. R.; Manners, I. *Mater. Today* **2008**, *11*, 28–36. (b) Wolf, M. O. *J. Inorgan. Organomet. Polym. Mater.* **2006**, *16*, 189–199.

10.1021/ja104051x

disadvantage of Salen and related ligands is that the attachment of electroactive, polymerizable substituents, such as thiophene or bithiophene, is challenging due to the coupling chemistry required.[9] Moreover, the rigid geometry of the resulting Salen ligand constrains the coordinated metal to a tight, four-coordinate environment which can complicate further derivatization.

Given the widespread use of α-diimines for the support of a significant variety of p-, d-, and f-block functionalities, we were prompted to develop a new electropolymerizable ligand class via the attachment of flanking thiophene substituents to an α-diimine. Such a system was envisioned to create a more open site for metal coordination and also to avoid the use of the aforementioned coupling reactions. Although our initially synthesized diimine ligand, 1,2(bis)-thiophene diazadiene met these requirements, it failed to undergo electropolymerization under reasonable conditions.[10,11] To overcome this limitation, the thiophene moieties in this substrate were replaced with bithiophenes, and the ligand was incorporated into an N-heterocyclic carbene (NHC) scaffold.

NHCs have attracted considerable attention over the last two decades due to their ability to stabilize many transition metal and main group complexes under a wide range of conditions.[12] Furthermore, polymeric materials have been shown to possess superior stabilities and enhanced electrocatalytic kinetics when compared with their monomeric analogues.[13−16] Although many examples are known in which NHCs have been incorporated into the backbones of polymeric materials,[16] no examples existed until very recently of polymers in which the NHCs were

Scheme 1. Synthesis of Gold NHC Complex **4**

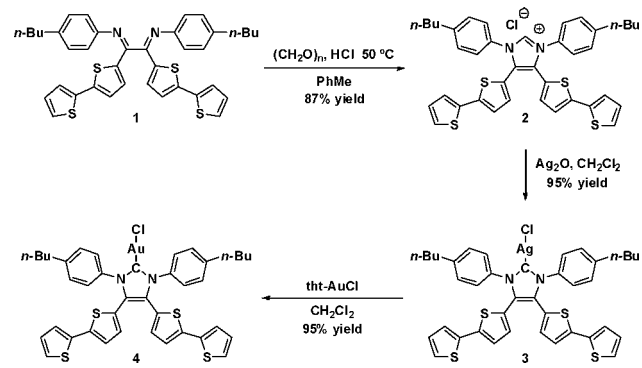

Scheme 2. Electrochemical Polymerization of Bithiophene-Substituted NHC−Metal Complexes **3**−**8**

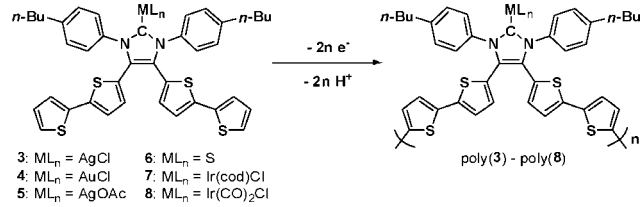

positioned orthogonally with respect to the main chains and thus available for ligation to other functionalities.[17] As summarized in Scheme 1, the requisite monomer for accessing such main-chain poly(NHC)s was synthesized by the cyclization of diimine **1** to form the corresponding imidazolium chloride **2**. Subsequent metalation of **2** with Ag_2O (to form **3**) followed by transmetallation with tetrahydrothiophene (tht)AuCl (tht = tetrahydrothiophene) afforded **4**, which was subsequently electropolymerized and characterized using standard techniques.[17]

Inspired by a recent account which demonstrated the impact of different coordinated metals on the electronic behavior of ECPs,[18] we have undertaken a comprehensive investigation of the influence of the ligated metal centers on the electronic properties of the aforementioned main-chain poly(NHC) complexes. More specifically, the methodology detailed for the gold NHC polymer was expanded to include polymers containing other transition metal and main group moieties (see Scheme 2), which were characterized using a suite of electrochemical, X-ray photoelectron and UV−vis spectroscopy, profilometry, and four-point probe conductivity measurements.

During the course of these studies, a noticeable color change was observed when the gold NHC complex **4** was electropolymerized on an indium tin oxide (ITO) slide. It was surmised that this change originated from the development of polarons along the polymer main chains. In general, polymers such as poly(3,4-ethylenedioxythiophene) (PEDOT) are well-known to exhibit such electrochromic characteristics, but examples of organometallic-based ECPs are relatively rare.[18] Electro-

(9) (a) Sauvage, J. P.; Kern, J. M.; Bidan, G.; Divisia-Blohorn, B.; Vidal, P. L. *New J. Chem.* **2002**, *26*, 1287–1290. (b) Jousselme, B.; Blanchard, P.; Ocafrain, M.; Allain, M.; Levillain, E.; Roncali, J. *J. Mater. Chem.* **2004**, *14*, 421–427.

(10) Powell, A. B.; Brown, J. R.; Vasudevan, K. V.; Cowley, A. H. *Dalton Trans.* **2009**, *14*, 2521–2527.

(11) Interestingly, a recent publication revealed a similar outcome for electropolymerizable phosphine-substituted monomers, see: Velauthamurty, K.; Higgins, S. J.; Rajapakse, R. M. G.; Bacsa, J.; van Zalinge, H.; Nichols, R. J.; Haiss, W. *J. Mater. Chem.* **2009**, *19* (13), 1850–1858.

(12) (a) Radloff, C.; Hahn, F. E.; Pape, T. *Frölich Dalton Trans.* **2009**, *35*, 7215–7222. (b) Hahn, F. E.; Radloff, C.; Pape, T.; Hepp, A. *Organometallics* **2008**, *27*, 6408–6410. (c) Karimi, B.; Akhaven, P. F. *Chem. Commun.* **2009**, *25*, 3750–3752. (d) Bartolome, C.; Ramiro, Z.; Garcia-Cuadrado, D.; Pérez-Galán, P.; Raducan, M.; Bour, C.; Echavarren, A. M.; Espinet, P. *Organometallics* **2010**, *29*, 951–956. For recent reviews see: (e) Diez-Gonzalez, S.; Marion, N.; Nolan, S. P. *Chem. Rev.* **2009**, *109*, 3612–3676. (f) Lin, J. C. Y.; Huang, R. T. W.; Lee, C. S.; Bhattacharyya, A.; Hwang, W. S.; Lin, I. J. B. *Chem. Rev.* **2009**, *109*, 3561–3598. (g) Kühl, O. *Chem. Soc. Rev.* **2007**, *36*, 592–607. (h) Arnold, P. L.; Pearson, S. *Coord. Chem. Rev.* **2007**, *251* (5−6), 596–609.

(13) Winter, A.; Friebe, C.; Chiper, M.; Hager, M. D.; Schubert, U. S. *J. Polym. Sci., Part A* **2009**, *47*, 4083–4098.

(14) Leung, A. C. W.; Chong, J. H.; MacLachlan, M. J. *Macromol. Symp.* **2003**, *196*, 229–234.

(15) Malinauskas, A. *Synth. Met.* **1999**, *107*, 75–83.

(16) (a) Boydston, A. J.; Williams, K. A.; Bielawski, C. W. *J. Am. Chem. Soc.* **2005**, *127*, 12496–12497. (b) Kamplain, J. W.; Bielawski, C. W. *Chem. Commun.* **2006**, *16*, 1727–1729. (c) Boydston, A. J.; Rice, J. D.; Sanderson, M. D.; Dykhno, O. L.; Bielawski, C. W. *Organometallics* **2006**, *25*, 6087–6098. (d) Boydston, A. J.; Bielawski, C. W. *Dalton Trans.* **2006**, 4073–4077. (e) Catalano, V. J.; Etogo, A.O. *Inorg. Chem.* **2007**, *46*, 5608–5615. (f) Karimi, B.; Akhavan, P. F. *Chem. Commun.* **2009**, *25*, 3750–3752. (g) Coady, D. J.; Kharmov, D. M.; Norris, B. C.; Tennyson, A. G.; Bielawski, C. W. *Angew. Chem., Int. Ed.* **2009**, *48*, 5187–5190. (h) Mercs, L.; Neels, A.; Stoeckli-Evans, H.; Albrecht, M. *Dalton Trans.* **2009**, *35*, 7168–7178. (i) Chiu, P. L.; Chen, C. Y.; Zeng, J. Y.; Lu, C. Y.; Lee, H. M. *J. Organomet. Chem.* **2005**, *690* (6), 1682–1687. (j) Guerret, O.; Solé, S.; Gornitzka, H.; Teichert, M.; Trinquier, G.; Bertrand, G. *J. Am. Chem. Soc.* **1997**, *119*, 6668–6669. (k) Norris, B. C.; Bielawski, C. W. *Macromolecules* **2010**, *43*, 3591–3593.

(17) Powell, A. B.; Bielawski, C. W.; Cowley, A. H. *J. Am. Chem. Soc.* **2009**, *131*, 18232–18233.

(18) Farrell, J. R.; Lavoie, D. P.; Pennell, R. T.; Cetin, A.; Shaw, J. L.; Ziegler, C. J. *Inorg. Chem.* **2007**, *46*, 6840–6842.

(19) (a) Padilla, J.; Seshadri, V.; Sotzing, G. A.; Otero, T. F. *Electrochem. Commun.* **2007**, *9*, 1931–1935. (b) Mecerreyes, D.; Marcilla, R.; Ochoteco, E.; Grande, H.; Pomposo, J. A.; Vergaz, R.; Sánchez Pena, J. M. *Electrochem. Acta* **2004**, *49*, 3555–3559. (c) Granqvist, C. G.; Azens, A.; Isidorsson, J.; Kharrazi, M.; Kullman, L.; Lindstroem, T.; Niklasson, G. A.; Ribbing, C.-G.; Roennow, D.; Stromme Mattson, M.; Veszelei, M. *J. Non-Cryst. Solids* **1997**, *218*, 273–279.

chromism is a useful property that has found commercial applications in color-changing windows and mirrors,[19] polymer light-emitting diodes,[20] and near-infrared (NIR) devices.[21] Moreover, there is a current demand for organic materials which exhibit excellent color efficiencies and fast switching capabilities.[22] On a different level, the study of electrochromic materials is also useful for analysis of the electronic structures of *p*-doped conjugated polymers in both the oxidized (cationic) and reduced (neutral) states.[23] The metallopolymer scaffolds shown in Scheme 2 are well suited for use in electrochromic devices since they: (1) should enable coordination of a range of transition metals and main group elements, each of which may display different characteristics, and (2) feature orthogonally positioned carbene groups in direct electronic contact with the polymerizable scaffold, which may be further derivatized to tailor the electronic properties exhibited by the materials in which they are contained.

Experimental Section

General Procedures. All solvents and reagents were used as received from commercial sources unless stated otherwise. The synthesis of the bithiophene-substituted diimine **1** and imidazolium chloride **2** are reported elsewhere.[17] Methylene chloride was distilled over calcium hydride prior to use. NMR spectra were recorded at 298 K on a Varian Inova instrument (^{1}H NMR, 499.40 MHz; ^{13}C NMR, 125.57 MHz) using residual solvent or tetramethylsilane (TMS) as an internal reference unless stated otherwise. Low-resolution chemical ionization mass spectral data (MS-CI) were collected on a Thermo Scientific TSQ Quantum GC mass spectrometer. High-resolution CI-MS spectra were recorded on a magnetic sector Waters Autospec Ultima instrument or on an IonSpec 9.4T FT mass spectrometer equipped with an ESI source, and data are reported as *m*/*z* (relative intensity). Infrared spectra were recorded in the solid state (KBr) using a Nicolet Avatar 260 FT-IR spectrometer. The spectroelectrochemical and absorbance measurements were recorded on a Varian Cary 5000 UV−vis−NIR spectrophotometer using Starna quartz fluorometer cells with a path length of 10 mm for **3** and **5**−**8** and a 0.1 mm path length for poly(**3**)−poly(**8**).

Electrochemistry. Electrochemical syntheses and studies were performed in a glovebox under a nitrogen atmosphere using a CH Instruments Electrochemical Workstation (series 700B). All electrochemical experiments were carried out in a three-electrode cell consisting of a platinum button working electrode, a tungsten counter-electrode, and a silver wire pseudoreference electrode. A 0.1 M solution of [(*n*-Bu)$_4$N$^+$][PF$_6^-$] (TBAPF$_6$) was used as the supporting electrolyte. The TBAPF$_6$ was purified via recrystallization three times from hot ethanol before being dried for 3 days at >100 °C under a dynamic vacuum. Electrosyntheses of the films onto a platinum button were performed from 1×10^{-3} M monomer solutions by continuous cycling between −0.20 and 1.50 V (upper limit of 1.70 V for **6**) at $\nu = 100$ mV s^{-1}. Analogous continuous cycling was performed between −0.20 V and +1.70 V for deposition of the polymers onto either stainless steel or ITO slides. The resulting films were then washed with copious amounts of CH_2Cl_2 and stored in the absence of light. All potentials listed in the manuscript and Supporting Information were referenced to SCE by shifting Fc*^{0}/Fc*$^+$ to −0.057 V.[24]

Spectroelectrochemistry. Spectroelectrochemical data were recorded on a Varian Cary 5000 UV−vis−NIR spectrophotometer using Starna quartz cells. A three-electrode cell was constructed in which each polymer was deposited onto a ITO-coated glass and used as the working electrode. The counter- and pseudoreference electrodes consisted of tungsten and silver wires, respectively, using 0.1 M TBAPF$_6$ in CH_2Cl_2 solution. An Eco Chemie Autolab PGSTAT30 equipped with GPES software was used to adjust the potential of the three-electrode cell in the UV−vis spectrophotometer. The polymers that were deposited onto the ITO electrodes were analyzed using UV−vis−NIR spectroscopy (1600 nm−300 nm) while increasing the voltage in stepwise intervals of 0.10 V, from 0.00 to 1.50 V. The stability of each film was determined by continuous cycling at 0.10 V/s until the electrochromic signal observed at approximately 700 nm decreased to 50% of its initial absorbance.

X-ray Photoelectron Spectroscopy. All XPS spectra were recorded on a Kratos Axis Ultra X-ray photoelectron spectrometer utilizing a monochromated Al Kα X-ray source ($h\nu = 1486.5$ eV), hybrid optics (employing a magnetic and electrostatic lens simultaneously), and a multichannel plate and delay line detector coupled to a hemispherical analyzer. The photoelectron takeoff angle of 0° (measured from the surface normal) was used in all experiments. All spectra were recorded using an aperture slot of 300 × 700 μm, and the high resolution spectra were collected with a pass energy of 20 eV. The pressure in the analysis chamber was typically held at 2×10^{-9} Torr during data acquisition. Kratos XPS analysis software was used to determine the stoichiometries of the samples from the corrected peak areas by applying the appropriate sensitivity factors for each element of interest. All reported ratios represent the average of two independent sample acquisitions, and all binding energies are reported with respect to the carbon 1s signal at 286.1 eV.

X-ray Crystallography. All crystals were grown in the absence of light. Crystals suitable for data collection were covered with hydrocarbon oil and mounted on thin nylon loops. The X-ray diffraction data were collected at 153 K on a Rigaku AFC-12 diffractometer equipped with a Saturn 724 and CCD area detector, an Oxford Cryostream low-temperature device, and a graphite-monochromated Mo Kα radiation source ($\lambda = 0.71073$ Å). Corrections were applied for Lorentz and polarization effects. The structures were solved by direct methods and refined by full-matrix least-squares cycles on F^2.[25] All non-hydrogen atoms were refined with anisotropic thermal parameters, and all hydrogen atoms were placed in fixed, calculated positions using a riding model (C−H, 0.96 Å).

Profilometry and Conductivity. Profilometry measurements for **3**−**8** were performed on a Dektak 6 M Stylus Profilometer in a clean-room facility. The average thicknesses of the polymers were based on an average of 12 data acquisitions on two different samples. The samples were prepared by electropolymerizaton of the polymers on ITO slides using cyclic voltammetry (50 cycles) between −0.2 V and +1.7 V.

Bithiophene-Substituted Silver NHC Complex 3. The imidazolium chloride **2**[17] (0.115 mmol, 0.080 g) and silver(I) oxide (0.069 mmol, 0.016 g) were added to a round-bottomed flask containing dry CH_2Cl_2 (15 mL), and the flask was covered with aluminum foil. The reaction mixture was stirred at ambient temperature for 48 h in the absence of light, after which it was filtered through Celite. The solvent was removed under reduced pressure to afford the desired product **3** as a yellow solid (95% yield). Single crystals suitable for X-ray data collection were obtained by slow vapor diffusion of hexanes into a solution of **3** in THF (1:3.00 THF:hexanes v/v) over a period of five days at ambient temperature. ^{1}H NMR (499.40 MHz, CD_2Cl_2, TMS): δ 7.28 (d, 4H, $J = 8.0$ Hz), 7.22 (d, 4H, $J = 8.0$ Hz) 7.15 (dd, 2H, $J = 5.0$, 1.0 Hz), 7.00 (dd, 2H, $J = 3.5$, 1.0 Hz), 6.90−6.88 (m, 4H), 6.69 (d, 2H, $J = 3.5$

(20) Mortimer, R. G. *Chem. Soc. Rev.* **1997**, *26*, 147–156.
(21) (a) Sonmez, H.; Meng, H.; Wudl, F. *Chem. Mater.* **2003**, *15*, 4923–4929. (b) Meng, H.; Tucker, S.; Chaffins, Y.; Chen, R.; Helgeson, R.; Dunn, B.; Wudl, F. *Adv. Mater.* **2003**, *15*, 146–149.
(22) Kraft, A.; Grimsdale, A. C.; Holmes, A. B. *Angew. Chem., Int. Ed.* **1998**, *37*, 403–428.
(23) Pang, Y.; Li, X.; Ding, H.; Shi, G.; Jin, L. *Electrochim. Acta* **2007**, *52*, 6172–6177.
(24) Noviadri, I.; Brown, K. N.; Fleming, D. S.; Gulyas, P. T.; Lay, P. A.; Masters, A. F.; Phillips, L. *J. Phys. Chem. B* **1999**, *103*, 6713–6722.
(25) Sheldrick, G. M. *SHELL-PC*, version 5.03; Siemens Analytical X-ray Instruments, Inc.: Madison, WI, 1994.

Hz), 2.60 (t, 4H, $J = 7.5$ Hz), 1.55 (quint, 4H, $J = 7.0$ Hz), 1.29 (sextet, 4H, $J = 7.5$ Hz), 0.85 (t, 6H, $J = 7.0$ Hz). $^{13}C\{^1H\}$ NMR (125.57 MHz, CD_2Cl_2): δ 145.38, 141.22, 136.40, 136.22, 132.15, 129.81, 128.32, 127.50, 127.43, 126.01, 125.73, 124.81, 123.80, 35.39, 33.60, 22.73, 14.06. The carbenoid carbon was detected when $CDCl_3$ was used as the solvent: $^{13}C\{^1H\}$ NMR (150.83 MHz, $CDCl_3$): δ 181.21(br). LRMS (CI^+ *m/z*): 804 (100% M + H^+). HRMS (CI^+, CH_4): calcd for $C_{39}H_{36}N_2S_4{}^{107}AgCl$, 802.0504; found, 802.0501. Calcd for $C_{39}H_{36}N_2S_4{}^{109}AgCl$, 804.0493; found, 804.0497. The bis-ligated silver cation was also detected. HRMS (ESI): calcd for $C_{78}H_{72}N_4S_8{}^{107}Ag$, 1427.25681; found, 1427.25317. IR (cm^{-1}): 3060, 2954, 2926, 2856, 1628 (C−C_{arom}), 1510 (C−C_{arom}), 1388, 1229, 1048, 1019, 838, 800, 696. $\lambda_{max} = 325$ nm. $\varepsilon = 4.9 \times 10^4$ M^{-1} cm^{-1}.

Bithiophene-Substituted Silver NHC Complex 5. The imidazolium chloride **2**[17] (0.057 mmol, 0.040 g) and silver(I) acetate (0.143 mmol, 0.024 g) were added to a round-bottomed flask containing 3 Å sieves and dry CH_2Cl_2 (15 mL). The reaction vessel was then covered with aluminum foil, and the reaction mixture was stirred at ambient temperature for 48 h in the absence of light. The reaction mixture was then filtered through Celite, and the solvent was removed under reduced pressure to afford the desired product **5** as a yellow solid (96% yield). Single crystals suitable for X-ray data collection were obtained after one week by layering a THF solution of **5** with hexanes at −40 °C (1:3 THF:hexanes v/v). ^1H NMR (400.27 MHz, $CDCl_3$, TMS): δ 7.29 - 7.20 (m, 8H), 7.16 (d, 2H, $J = 5.2$ Hz) 7.00 (d, 2H, $J = 4.0$ Hz), 6.91−6.88 (m, 4H), 6.68 (d, 2H, $J = 3.2$ Hz), 2.61 (t, 4H, $J = 7.6$ Hz), 1.81 (s, 3H), 1.56 (quint, 4H, $J = 8.4$ Hz), 1.30 (sextet, 4H, $J = 7.2$ Hz), 0.86 (t, 6H, $J = 7.2$ Hz). $^{13}C\{^1H\}$ NMR (125.57 MHz, CD_2Cl_2): δ 175.86, 144.06, 140.07, 135.30, 135.20, 131.01, 128.63, 127.19, 126.40, 126.27, 124.98, 124.58, 123.67, 122.66, 34.45, 32.48, 21.59, 21.47, 12.94. As in the cases of similar complexes, the carbenoid carbon could not be detected by ^{13}C NMR spectroscopy.[26] LRMS (CI^+ *m/z*): 661 (100% $M^+ + H^+ - AgC_2H_3O_2$), 828 (20% M + H^+). The bis-ligated silver cation was also detected. HRMS (ESI): calcd for $C_{78}H_{72}N_4S_8{}^{107}Ag$, 1427.25681; found, 1427.25771. IR (cm^{-1}): 3067, 2954, 2927, 2858, 1578 (C−C_{arom}), 1510 (C−C_{arom}), 1382, 1327, 1018, 838, 804, 696. $\lambda_{max} = 325$ nm. $\varepsilon = 3.0 \times 10^4$ M^{-1} cm^{-1}.

Bithiophene-Substituted Thione 6. The imidazolium chloride **2**[17] (0.143 mmol, 0.100 g), elemental sulfur (0.179 mmol, 0.006 g) and K_2CO_3 were added to a Schlenk flask. Degassed MeOH (25 mL) was then added *via* cannula to the reaction mixture, which was stirred subsequently at ambient temperature for 24 h. The product was then extracted into CH_2Cl_2 (50 mL) and washed with water (3 × 25 mL). The aqueous layer was back-extracted and organic layers combined. The organic layer was then dried with $MgSO_4$, filtered and concentrated to afford the desired product **6** as an orange solid (98% yield). Single crystals suitable for X-ray data collection were obtained after three days by the slow vapor diffusion of hexanes into a solution of **6** in THF (1: 2.5 THF: hexanes v/v) at ambient temperature. ^1H NMR (499.40 MHz, CD_2Cl_2, TMS): δ 7.24 (d, 4H, $J = 8.5$ Hz), 7.21 (d, 4H, $J = 8.5$ Hz) 7.12 (dd, 2H, $J = 5.5$, 1.0 Hz), 6.96 (dd, 2H, $J = 3.5$, 1.0 Hz), 6.96 (dd, 2H, $J = 5.0$, 1.5 Hz), 6.83 (d, 2H, $J = 3.5$ Hz), 6.62 (d, 2H, $J = 4.0$ Hz), 2.58 (t, 4H, $J = 7.5$ Hz), 1.55 (quint, 4H, $J =$ Hz), 1.27 (sextet, 4H, $J = 7.5$ Hz), 0.84 (t, 6H, $J = 7.0$ Hz). $^{13}C\{^1H\}$ NMR (125.57 MHz, CD_2Cl_2): δ 167.11, 144.67, 140.27, 136.63, 134.71, 131.50, 129.45, 129.17, 128.24, 127.14, 125.42, 124.52, 123.58, 123.36, 35.35, 33.66, 22.70, 14.07. LRMS (CI^- *m/z*): 692 (100% M^+). HRMS (CI^+, CH_4): calcd for $C_{39}H_{36}N_2S_5$, 693.15548; found, 693.15543. IR (cm^{-1}): 3067, 2956, 2928, 2857, 1510 (C−C_{arom}), 1385 (C−C_{arom}), 1344, 1229, 1048, 1019, 838, 800, 696. $\lambda_{max} = 324$ nm. $\varepsilon = 4.3 \times 10^4$ M^{-1} cm^{-1}.

Bithiophene-Substituted Iridium NHC Complex 7. The bithiophene-substituted silver NHC **3** (0.137 mmol, 0.110 g) and chloro(1,5-cyclooctadiene)iridium(I) dimer (0.075 mmol, 0.051 g) were added to a round-bottomed flask containing dry CH_2Cl_2 (15 mL), and the reaction vessel was covered with aluminum foil. The reaction mixture was stirred at ambient temperature for 72 h, after which it was filtered through Celite and the solvent was removed under reduced pressure to afford the desired product **7** as a brown powder (95% yield). ^1H NMR (499.40 MHz, CD_2Cl_2, TMS): δ 7.57 (d, 4H, $J = 8.0$ Hz), 7.16 (d, 4H, $J = 8.5$ Hz), 7.12 (dd, 2H, $J =$ 5.0, 1.0 Hz), 6.98 (dd, 2H, $J = 3.5$, 1.0 Hz), 6.87 (m, 4H), 6.71 (d, 2H, $J = 3.5$ Hz), 4.13 (m, 2H), 2.59 (t, 4H, $J = 7.0$), 2.50 (m, 2H), 1.56 (quint, 6H, $J = 7.5$ Hz), 1.27 (sextet, 8H, $J = 7.5$ Hz), 1.11 (m, 2H), 0.83 (t, 6H, $J = 7.5$ Hz). $^{13}C\{^1H\}$ NMR (125.57 MHz, CD_2Cl_2, TMS): δ 182.62, 142.87, 139.38, 135.54, 134.86, 130.83, 128.04, 127.41, 127.11, 125.94, 125.90, 124.31, 123.47, 122.51, 82.14, 50.75, 34.50, 32.75, 32.06, 28.09, 21.35, 12.94. LRMS (CI^+ *m/z*): 996 (100% $M^+ + H^+$), 959 (55% M − Cl). HRMS (CI^+, CH_4): calcd for $C_{47}H_{48}N_2ClS_4{}^{193}Ir$, 996.2024; found, 996.2018. IR (cm^{-1}): 3067, 2954, 2924, 2858, 1509 (C−C_{arom}), 1420 (C−C_{arom}), 1375, 1327, 1262, 1019, 837, 799, 689. $\lambda_{max} = 324$ nm. $\varepsilon = 4.2 \times$ 10^4 M^{-1} cm^{-1}.

Bithiophene-Substituted Iridium NHC Complex 8. Complex **7** was added to a round-bottomed flask containing dry CH_2Cl_2 (5 mL). The reaction vessel was then fitted with a rubber septum, and the solution was degassed. The resulting solution was stirred under an atmosphere of carbon monoxide for 12 h, after which it was filtered through Celite and the solvent was removed under reduced pressure to afford the desired product **8** as a brown powder (98% yield). ^1H NMR (499.40 MHz, CD_2Cl_2, TMS): δ 7.36 (d, 4H, $J =$ 8.5 Hz), 7.20 (d, 4H, $J = 8.5$ Hz), 7.12 (dd, 2H, $J = 5.0$, 1.0 Hz), 6.97 (dd, 2H, $J = 4.0$, 1.5 Hz), 6.86 (m, 4H), 6.65 (d, 2H, $J = 4.0$ Hz), 2.61 (t, 4H, $J = 5.0$ Hz), 1.57 (quint, 4H, $J = 8.0$ Hz), 1.28 (sextet, 4H, $J = 8.0$ Hz), 0.85 (t, 6H, $J = 7.5$ Hz). $^{13}C\{^1H\}$ NMR (125.57 MHz, CD_2Cl_2, TMS): δ 180.33, 174.44, 167.45, 144.14, 140.07, 135.28, 134.00, 130.94, 128.12, 127.98, 127.16, 126.84, 124.69, 124.55, 123.64, 122.62, 34.51, 32.39, 21.55, 12.97. LRMS (CI^+ *m/z*): 944 (20% M^+), 909 (100% M − Cl). HRMS (CI^+, CH_4): calcd for $C_{41}H_{36}N_2ClO_2S_4{}^{193}Ir$, 944.0978; found, 944.0974. IR (cm^{-1}): 2953, 2926, 2856, 2058 (C=O), 1974 (C=O), 1658, 1510 (C−C_{arom}), 1398 (C−C_{arom}), 1334, 1261, 1202, 1020. $\lambda_{max} = 326$ nm. $\varepsilon = 1.8 \times 10^4$ M^{-1} cm^{-1}.

Results and Discussion

Monomer Synthesis and Characterization. The monomers **3** and **5**−**8** were synthesized as summarized in Scheme 3; monomer **4** was prepared as previously described.[17] The precursor bithiophene-substituted diimine **1** was synthesized by sodium cyanide-catalyzed coupling of the requisite aldimine in DMF solution. Cyclization of **1** with paraformaldedyde afforded the anticipated imidazolium chloride **2** in 87% yield. The imidazolium proton was identified by ^1H NMR spectroscopy as a singlet at $\delta = 10.41$ ppm in CD_2Cl_2 solution. Access to silver NHC **3**, which has been previously utilized as a carbene transfer reagent,[17] was obtained by metalation of the requisite imidazolium chloride with Ag_2O. As reported for other silver NHC complexes,[27] an equilibrium was observed in solution between **3** and its dimeric analogue (see Scheme 4). As a consequence, the carbene nucleus of **3** could not be detected by ^{13}C NMR spectroscopy in CD_2Cl_2 solution. However, it was observed as a broad singlet at $\delta = 181$ ppm when the NMR spectrum was recorded in $CDCl_3$. In turn, this broad singlet resolved into two sets of doublets (in $CDCl_3$) at −50 °C, due to coupling of the ^{13}C nucleus to ^{107}Ag and ^{109}Ag with coupling constants of approximately 260 Hz. Related examples of this phenomenon have been reported previously for both silver

(26) Ogle, J. W.; Zhang, J.; Reibenspies, J. H.; Abboud, K. A.; Miller, S. A. *Org. Lett.* **2008**, *10*, 3677–3680.

(27) Newman, C. P.; Clarkson, G. J.; Rourke, J. P. *J. Organomet. Chem.* **2007**, *692*, 4962–4968.

Scheme 3. Syntheses of Monomers **3** and **5**−**8**

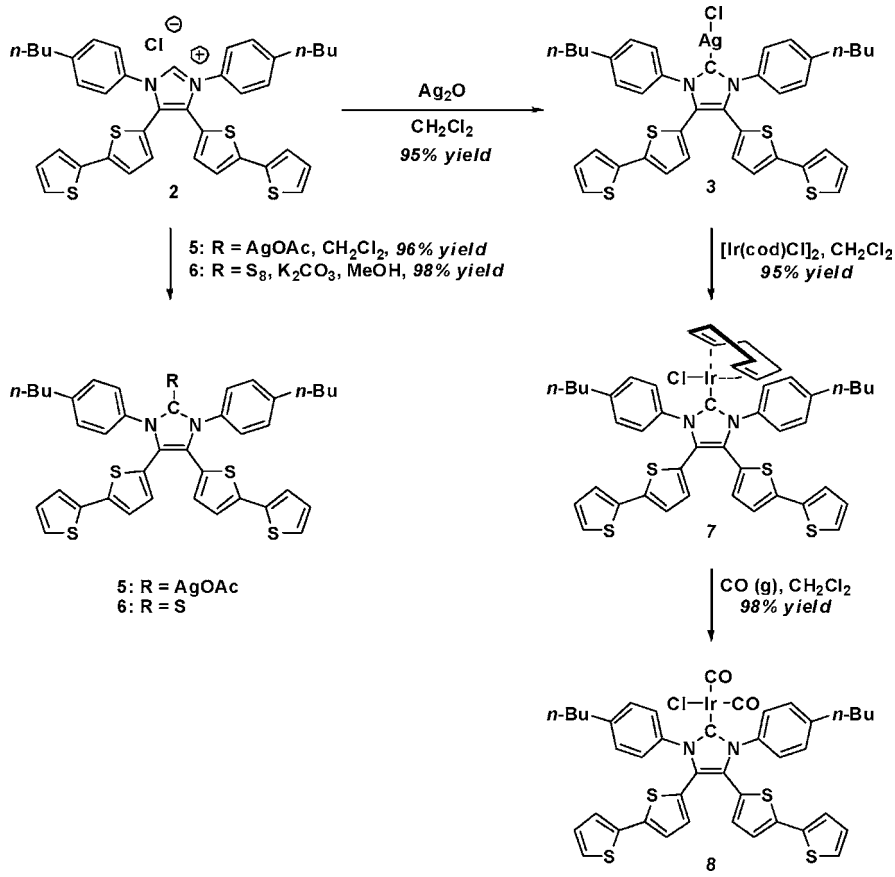

Scheme 4. Equilibrium Between **3** and a Dimeric Analogue

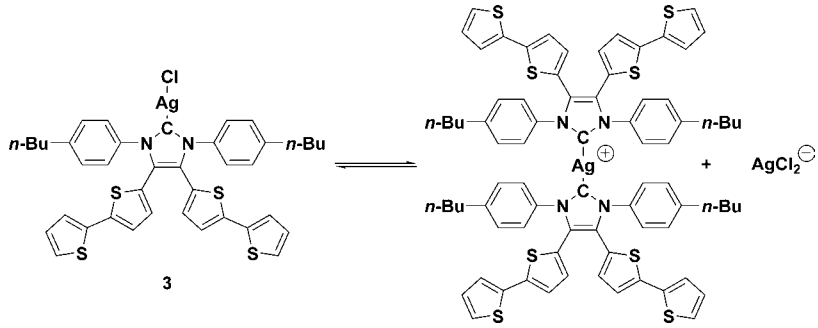

phosphine and silver carbene complexes.[28] Silver NHC **3** was also detected by double-sector high-resolution mass spectrometry, and the presence of a cationic complex consisting of the aforementioned complex featuring a Ag atom bound to two NHC ligands was evident from ESI spectrometry.

As shown in Figure 2 (left), a single-crystal X-ray diffraction experiment revealed the monomeric structure of **3**. Interestingly, the packing diagram exhibited a 1D array of metal atoms connected by short Ag−Ag contacts (Figure 2, right). The presence of these argentophilic interactions in silver carbene structures has been shown to be dependent upon the extent of steric crowding proximal to the metal center. For example, phenyl-substituted silver carbenes analogous to **3** exhibit comparable 1-D arrays of Ag−Ag contacts;[26] however, silver carbene analogues with bulky mesityl or diisopropylphenyl groups fail to do so in the solid state.[29] The distance between the carbene nucleus and the Ag atoms of **3** was measured to be 2.087(3) Å, a value that is significantly longer than the analogous carbon-metal 1.950(8) Å distance previously observed[17] for the gold NHC **4** as anticipated on the basis of relativistic effects.[30]

Attention was next directed toward the synthesis of the relatively bulky silver NHC **5** in order to discern whether the differences in solid state structure would affect the stabilities of the resulting polymers (see below). Complex **5** was synthesized in nearly quantitative yield by metalation of the precursor imidazolium chloride **2** with silver(I) acetate in CH_2Cl_2 solution.

(28) (a) Chen, F.; Oh, S. W.; Wasylishen, R. E. *Can. J. Chem.* **2009**, *87*, 1090–1101. (b) Ramnial, T.; Abernethy, C. D.; Spicer, M. D.; McKenzie, I. D.; Gay, I. D.; Clyburne, J. A. C. *Inorg. Chem.* **2003**, *42*, 1391–1393.

(29) Paas, M.; Wibbeling, B.; Fröhlich, R.; Hahn, F. E. *Eur. J. Inorg. Chem.* **2006**, *1*, 158–162.

(30) Bayler, A.; Schier, A.; Bowmaker, G. A.; Schmidbaur, H. *J. Am. Chem. Soc.* **1996**, *118*, 7006–7007.

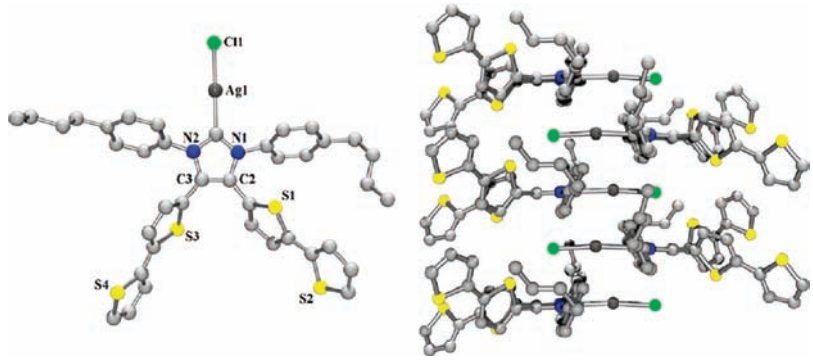

Figure 2. (left) POV-Ray view of **3** showing 50% probability thermal ellipsoids and selected atom labels. (right) Packing diagram for **3**. Hydrogen atoms have been omitted for clarity.

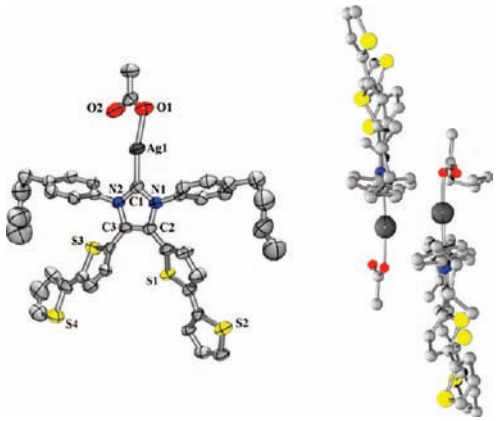

Figure 3. (left) POV-Ray view of **5** showing 50% probability thermal ellipsoids and selected atom labels. (right) Packing diagram for **5**. Hydrogen atoms have been omitted for clarity.

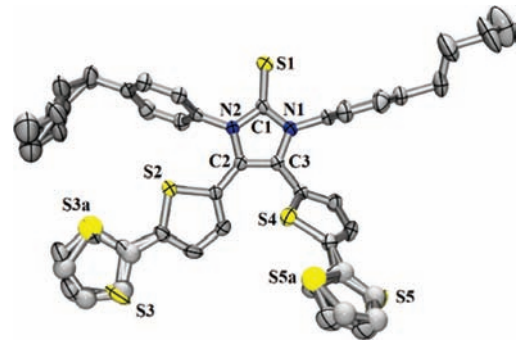

Figure 4. POV-Ray view of **6** showing 50% probability thermal ellipsoids and selected atom labels.

^{1}H NMR spectroscopic analysis revealed broad resonances for the phenyl groups, which suggested that this complex may exist in equilibrium with its dimeric counterpart, as observed in the case of **3**. Indeed, analysis by electrospray ionization (ESI) mass spectrometry revealed the presence of the diligated silver cation as shown in Scheme 4. Decomposition of **5** in solution was observed over the course of a few days, but slowed at lower temperatures. In contrast, **5** was found to be remarkably robust in the solid-state and was stored for several months under atmospheric conditions without noticeable decomposition. X-ray crystallographic analysis revealed that **5** was isolated as the monomeric silver carbene (Figure 3, left), replete with dimeric argentophilic interactions (Figure 3, right),[31] presumably due to the increased steric demands of the acetate ligand (in comparison with the chloride ligand in **3**).

Bithiophene-substituted iridium NHC complex **7** was synthesized by transmetalation of **3** with $[Ir(cod)Cl]_2$ (cod = 1,5-cyclooctadiene) in CH_2Cl_2 solution. In comparison with those of the starting material, the *ortho*-phenyl protons of **7** were shifted significantly downfield (δ = 7.27 to 7.57 ppm) as the reaction proceeded toward product. Furthermore, the vinyl protons of the cod ligand were split into two separate resonances, one at δ 2.50 (assigned to the olefin cis to the NHC) and the other at δ 4.15 (assigned to the olefin trans to the NHC) due to the stronger donating character of the NHC compared with that of the chloride ligand.[32] The iridium NHC complex **8** was synthesized by exposure of **7** to an atmosphere of carbon monoxide at ambient temperature for 12 h. Although solutions of **8** were unstable to prolonged storage as previously reported for other iridium NHC carbonyl complexes,[33] two IR absorptions were detected at ν_{CO} = 2058 and 1974 cm^{-1} corresponding to the two chemically distinct CO ligands.[34] The carbene ^{13}C NMR signal for **8** was detected at δ = 180 ppm (CD_2Cl_2) as a sharp singlet which is a similar value to that observed for **7** (δ = 183 ppm; CD_2Cl_2).

In parallel with the aforementioned metalation reactions, efforts were also directed toward the synthesis of a monomer that contained a main group element in lieu of a transition metal. As shown in Scheme 3, thione **6** was prepared via treatment of imidazolium chloride **2** with a mixture of S_8 and K_2CO_3 in methanol. The ^{13}C NMR resonance assigned to the thione carbon was observed at δ = 167 ppm (CD_2Cl_2), and the expected composition was confirmed by ESI mass spectrometry. Analysis of **6** via single-crystal X-ray diffraction provided additional support for the structure of this molecule (see Figure 4).[35]

Electropolymerization Studies. In general, the aforementioned complexes were independently electropolymerized in a three-electrode cell using a platinum button as the working electrode. The polymers synthesized from these reactions were obtained

(31) Lee, C. K.; Vasam, C. S.; Huang, T. W.; Wang, H. M. J.; Yang, R. Y.; Lee, C. S.; Lin, I. J. B. *Organometallics* **2006**, *25*, 3768–3775.

(32) Chang, Y. H.; Fu, C. F.; Liu, Y. H.; Peng, S. M.; Chen, J. T.; Liu, S. T. *Dalton Trans.* **2009**, 861–867.

(33) Ogle, J. W.; Miller, S. A. *Chem. Commun.* **2009**, *38*, 5728–5730.

(34) Bittermann, A.; Herdtweck, E.; Härter, P.; Herrmann, W. A. *Organometallics* **2009**, *28*, 6963–6968.

(35) (a) Türkmen, H.; Şahin, O.; Büyükgüngör, O.; Çetinkaya, B. *J. Inorg. Chem.* **2006**, *23*, 4915–4921. (b) Burford, N.; Phillips, A. D.; Spinney, H. A.; Robertson, K. N.; Cameron, T. S.; McDonald, R. *Inorg. Chem.* **2003**, *42*, 4949–4954.

as thin films and then characterized using a suite of electrochemical,[36] XPS,[37] UV−vis spectroscopy, profilometry, and four-point probe conductivity measurements.

The first monomer studied, the bithiophene-substituted diimine **1**, was successfully electropolymerized by continuous electrochemical cycling between −0.2 and +1.7 V. Although the current from the generated thin film of poly(**1**) was found to increase linearly with respect to the scan rate as expected,[38] the respective cyclic voltammogram of **1** revealed a reduction process near 0.0 V (see Supporting Information). For this reason, **1** was deemed unsuitable or coordinating various transition metals and forming metallopolymers. As described above, **1** was cyclized to form the imidazolium salt **2**, which was envisioned as a stable NHC precursor. Unfortunately, attempts to electropolymerize **2** were unsuccessful,[39] a likely consequence of the high oxidation potential of the monomer.

In contrast, the silver NHC complex **3**[17] was successfully electropolymerized under the aforementioned conditions. As shown in Figure 5 (top), the oxidation and reduction waves overlapped and the current measured increased in a linear fashion over 10 cycles. Cyclic voltammetry experiments conducted on a thin film of poly(**3**) revealed that, as expected, the current generated was directly proportional to the applied scan rate (see Figure 5, bottom).

To further characterize poly(**3**), its respective monomer was also electropolymerized onto stainless steel. Two distinct phases resulted, both of which were analyzed by XPS to determine their chemical compositions. One phase, which was visibly white in color, featured of a 1:1 molar ratio of silver to chlorine atoms. The lack of sulfur or nitrogen signals suggested to us that the bithiophene-substituted NHC moiety was absent. By inference, silver chloride had formed and was presumed to originate from the electrochemical oxidation of the $AgCl_2^-$ anion which is typically present in solutions of silver NHC complexes.[40] Analysis of the other phase, which was visibly yellow in color, revealed a S:Ag ratio of 3.70 and an N:Ag ratio of 1.83 (Table 1), values which were in agreement with the anticipated canonical structure of poly(**3**).[41] Moreover, when poly(**3**) was deposited onto an ITO slide, the yellow film exhibited a λ_{max} = 399 nm, a value that was red-shifted by 74 nm with respect to that measured for its monomer and consistent with the formation of an electronically delocalized polymeric structure.

Although poly(**3**) was successfully synthesized, subsequent efforts focused on the silver NHC acetate complex **5**, a monomer whose electropolymerization characteristics were predicted to not entail competitive or deleterious processes.[42] Using the method described above, electropolymerization of **5** afforded a thin film that was measured to be 1173 nm thick by profilometry. As shown in Figure 6 (top), a series of cyclic voltammetry experiments revealed that the oxidation current observed at 0.8 V increased along with the anticipated potential shifts following each subsequent cycle. The oxidation and reduction waves assigned to the polymer were clearly delineated from those of the monomer. Moreover, the current generated by oxidizing or reducing poly(**5**) was directly related to the scan rate up to 100 mV/s (Figure 6, bottom).

XPS examination of a thin film of poly(**5**) revealed that the ratios of the Ag, N, and S atoms were in accord with the

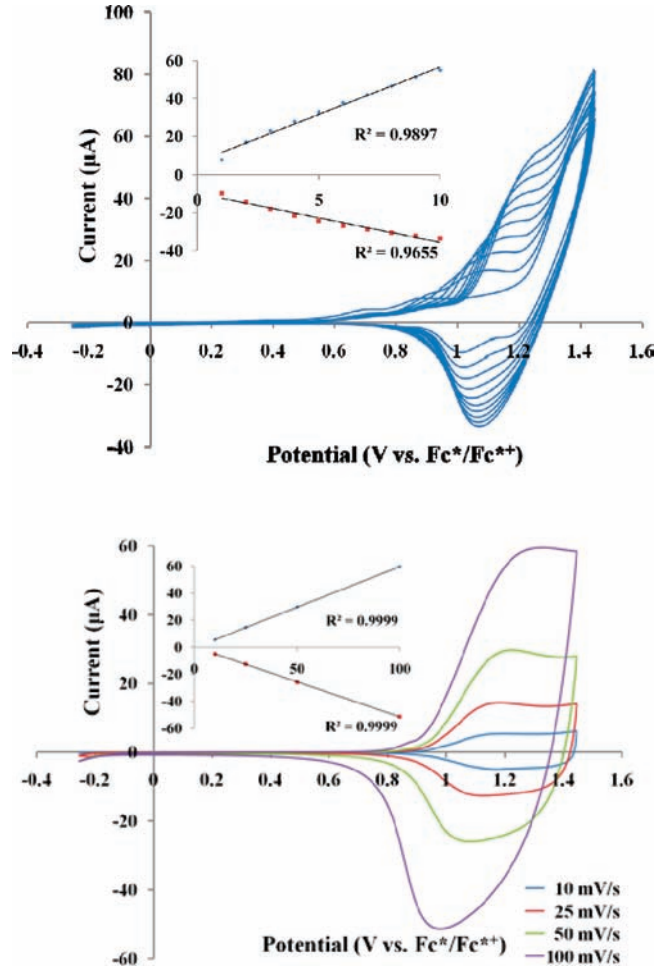

Figure 5. (top) Overlay of continuous cyclic voltammograms of silver NHC **3** over time. Inset: plot of current maxima vs number of cycles. (bottom) Cyclic voltammogram of thin film poly(**3**) at different scan rates. Inset: plot of current vs scan rate.

Table 1. Selected Properties of the Thin Films Prepared

poly.	ML_n	λ_{red}[a] (nm)	λ_{ox}[b] (nm)	stability[c] (cycles)	thickness[d] (nm)
poly(**3**)	AgCl	399			558
poly(**4**)	AuCl	392	702	35	348
poly(**5**)	AgOAc	395	677	12	1173
poly(**6**)	S	367	687	20	126
poly(**7**)	Ir(cod)Cl	333	704	30	294
poly(**8**)	$Ir(CO)_2Cl$	374	692[e]	50	750

[a] Absorbance maxima at 0.0 V. [b] Absorbance maxima for the signal attributed to polaron formation. [c] Stability was defined as the number of cycles (listed) observed until half of the absorbance peak measured near 700 nm was depleted. [d] Determined by profilometry. [e] An absorption at 1092 nm was observed and attributed to bipolaron formation.

(36) Scan rates for poly(**3**)−poly(**8**) above 100 mV/s resulted in distortions of the electrochemical profiles due to kinetic limitations on the counterion diffusion in and out of the polymer matrix.
(37) XPS analysis of the monomers was unsuccessful due to their inability to form thin films.
(38) The diimine thin film poly(**1**) could not be deposited on either stainless steel or ITO glass for further characterization.
(39) The cyclization succeeded in eliminating the reduction of the diimine moiety, but thin films of poly(**2**) were not detected on the electrode in monomer-free solutions.
(40) de Frémont, P.; Scott, N. M.; Stevens, E. D.; Ramnial, T.; Lightbody, O. C.; MacDonald, C. L. B.; Clyburne, J. A. C.; Abernethy, C. D.; Nolan, S. P. *Organometallics* **2005**, *24*, 6301–6309.
(41) Hesse, R.; Streubel, P.; Szargan, R. *Surf. Interface Anal.* **2005**, *37*, 589–607.
(42) For a recent review see: Hindi, K. M.; Panzner, M. J.; Cannon, C. L.; Youngs, W. J. *Chem. Rev.* **2009**, *109*, 3859–3884.

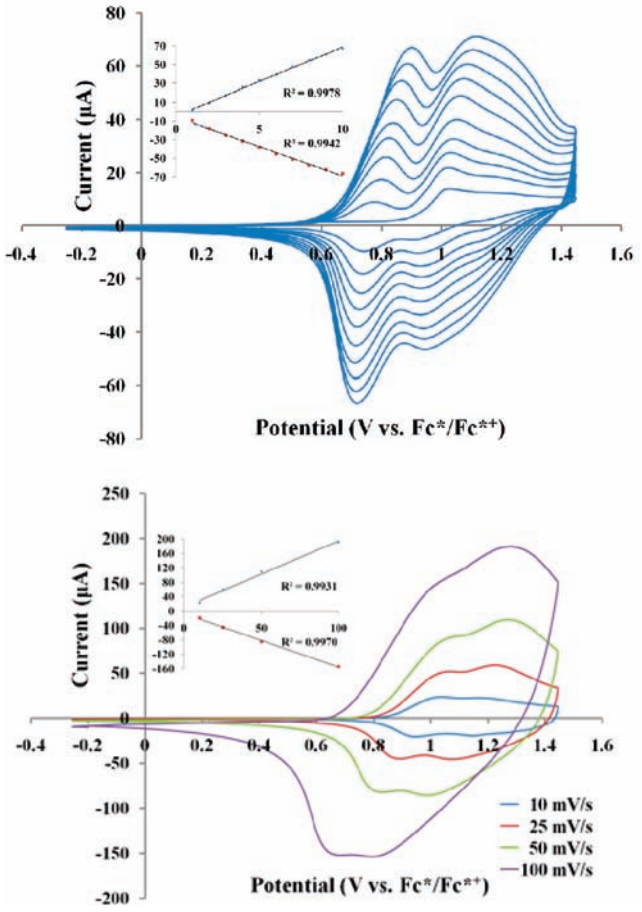

Figure 6. (top) Overlay of continuous cyclic voltammograms of silver NHC **5** over time. Inset: plot of current maxima vs number of cycles. (bottom) Cyclic voltammogram of thin film poly(**5**) at different scan rates. Inset: plot of current vs scan rate.

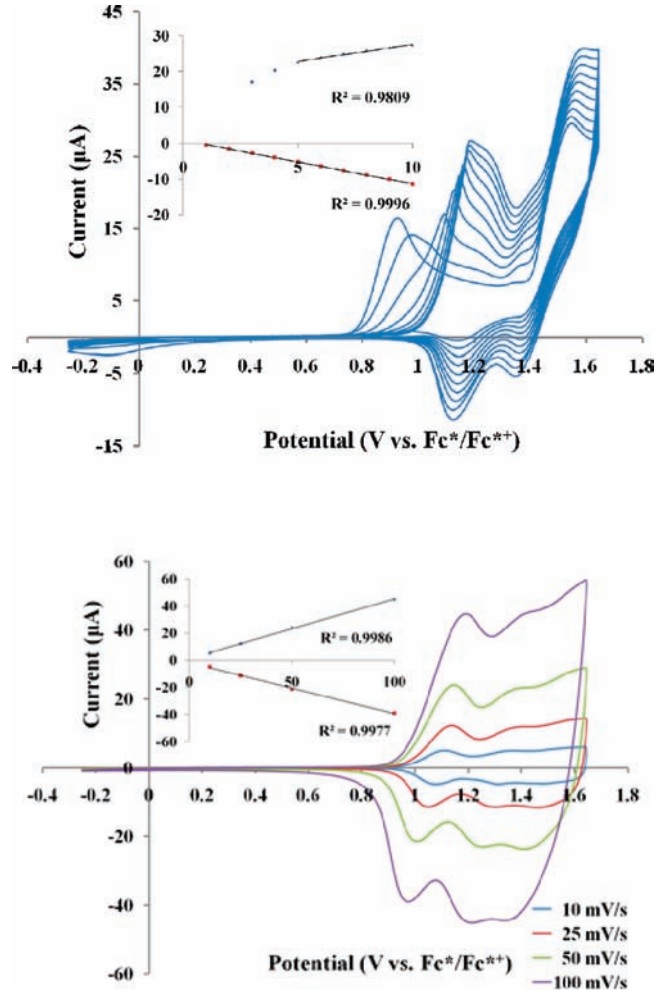

Figure 7. (top) Overlay of continuous cyclic voltammograms of thione **6** over time. Inset: plot of current maxima vs number of cycles. (bottom) Cyclic voltammogram of poly(**6**) at different scan rates. Inset: plot of current vs scan rate.

anticipated structure of this material. As predicted,[43] the silver 3d core electrons of poly(**5**) was measured to possess a binding energy of 368.6 eV, which is significantly higher than that measured for poly(**3**) (367.4 eV). The UV−vis spectrum of poly(**5**) also exhibited a strong bathochromic shift of 69 nm when compared to that measured for its respective monomer. In agreement with the results described above, this observation is consistent with the formation of an electronically delocalized polymeric structure.

Electropolymerization of the thione **6** was accomplished in a similar fashion to the analogous electrochemical experiments described above. As shown in Figure 7 (top), the maximum oxidation current was observed at 1.15 V, which is a higher potential than those observed for the other polymers analyzed thus far. In the first three electrochemical cycles, an oxidation was also detected near 0.9 V. Previous reports have suggested that this feature represents the oxidative attachment of the thione sulfur onto the platinum button[44] and that the accompanying reduction wave (−0.1 V) reflects detachment. After the first three cycles, however, poly(**6**) was observed to coat the surface of the electrode, which in turn prevented any further thione attachment.[45] As shown in Figure 7 (bottom), the current generated by poly(**6**) was also found to increase linearly with the scan rate up to 100 mV/s.

XPS analysis of poly(**6**) on a stainless steel substrate revealed a S:N ratio of 2.52, which is in close agreement with the expected value of 2.50. This observation provided additional evidence that **6** did not decompose during polymerization and that the anticipated structure of the polymer had formed. Examination of the UV−vis spectrum of this material revealed a $\lambda_{max} = 367$ nm, a value which is bathochromically shifted by 43 nm in comparison with that of the corresponding monomer.

The bithiophene-substituted iridium NHC **7** was electropolymerized next, and the plot of current versus potential is displayed in Figure 8 (top). In accord with related systems, a quasi-reversible oxidation of the metal center was measured at a potential of 0.75 V and the corresponding reduction peak was measured at 0.60 V.[46] Both of these electrochemical features decreased rapidly in intensity with repeated cycling and were no longer present after five cycles. Since a similar observation was made for the thin film poly(**6**), it was concluded that coating

(43) Moulder, J. F.; Stickle, W. F.; Sobol, P. E.; Bomben, K. *Handbook of X-ray Photoelectron Spectroscopy*, 2nd ed.; Perkin-Elmer: Eden Prarie, 1992.

(44) Bates, J. R.; Kathirgamanathan, P.; Miles, R. W. *Thin Solid Films* **1997**, *299*, 18–24.

(45) To support this argument, the thione analogue of the Kuhn carbene was synthesized, analyzed by cyclic voltammetry, and shown to possess similar electrochemical features as described in the literature for other thione compounds. The electrochemistry of the Kuhn thione is shown in the Supporting Information.

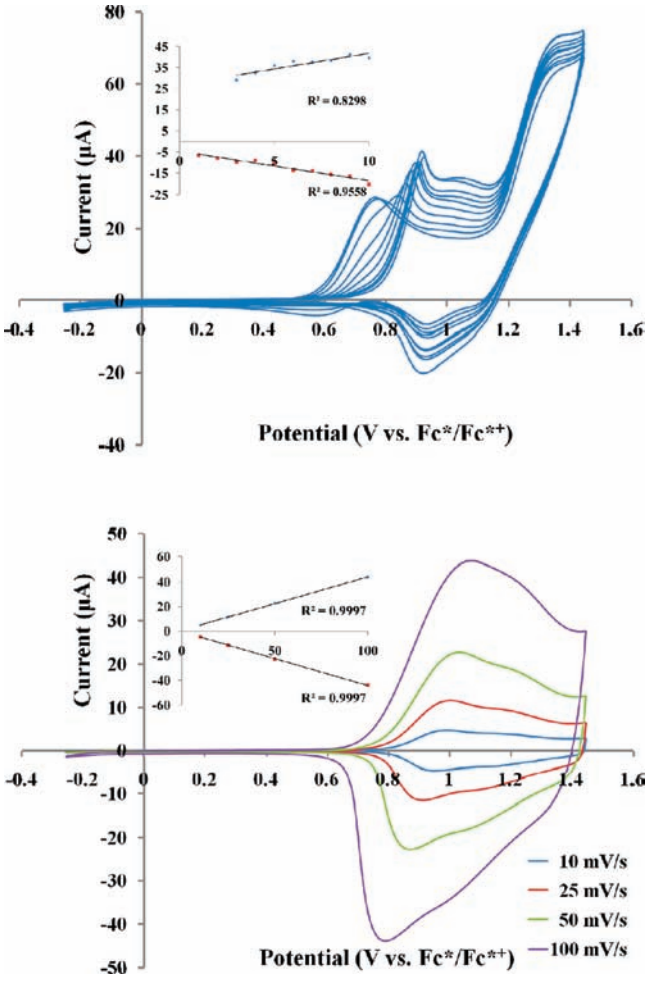

Figure 8. (top) Overlay of continuous cyclic voltammograms of iridium NHC **7** over time. Inset: plot of current maxima vs number of cycles. (bottom) Cyclic voltammogram of thin film poly(**7**) at different scan rates. Inset: plot of current vs scan rate.

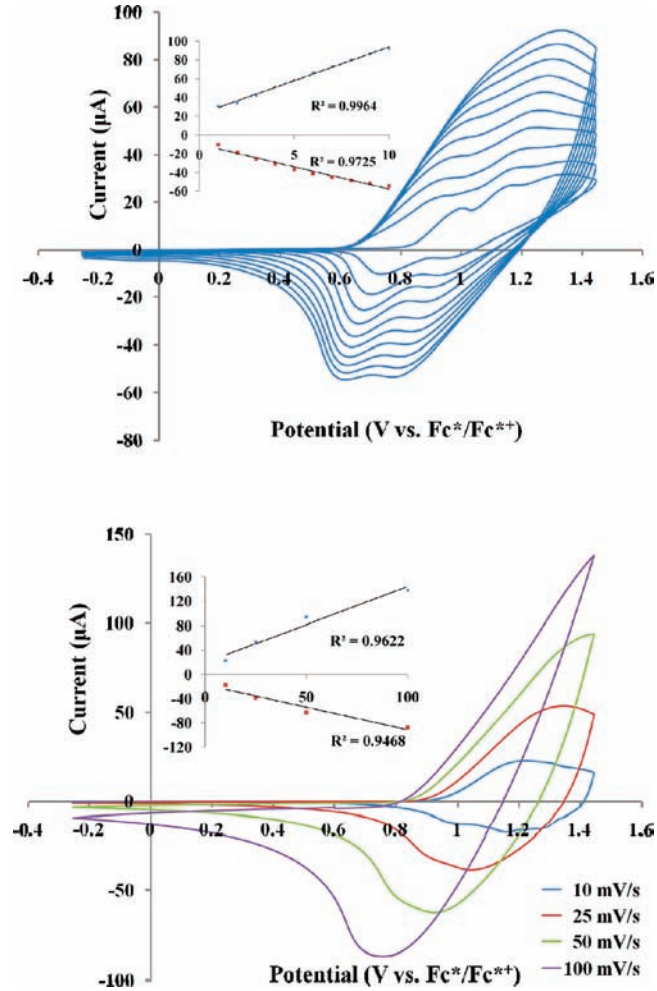

Figure 9. (top) Overlay of continuous cyclic voltammograms of iridium NHC **8** over time. Inset: plot of current maxima vs number of cycles. (bottom) Cyclic voltammogram of thin film poly(**8**) at different scan rates. Inset: plot of current vs scan rate.

of the electrode by poly(**7**) was responsible for this phenomenon. A linear relationship between current increase and number of consecutive cycles was not evident due to the concurrent oxidation of the coordinated iridium metal. Moreover, the metal oxidation process could not be detected by electrochemical cycling of poly(**7**) (Figure 8, bottom) in monomer-free solution, thus suggesting that the metal may not be present in the polymeric thin film. Related iridium-containing polymers, however, have been shown to lack a metal-centered oxidation process.[47] Hence, to gain additional insight into the composition of poly(**7**), the material was analyzed by XPS which revealed that the iridium, sulfur, and nitrogen atoms were present in the expected ratios. Surprisingly, the λ_{max} of the polymer was found to be only slightly red-shifted (9 nm) with respect to its monomer, which suggested to us that the film consisted primarily of oligomers of **7**.

To minimize the concurrent oxidation of the metal center during electropolymerization, the cod ligand of **7** was displaced with carbon monoxide since the latter is expected to anodically shift the oxidation potential of iridium NHC complexes. During the electropolymerization of iridium NHC **8** (Figure 9, top), metal oxidation was observed to increase from 0.75 to 1.20 V. As a result, and in contrast to **7**, a linear relationship between the increase in polymer current and the number of electrochemical cycles was observed. Poly(**8**) also exhibited a $\lambda_{max} = 374$ nm, a value that is bathochromically shifted by 48 nm compared to its monomer, which is a significantly larger shift than that measured upon polymerization of iridium NHC **7**. The electrodeposited thin film poly(**8**) was therefore expected to be comprised of relatively high molecular weight polymers (and not oligomers). Electrochemical cycling at different scan rates revealed a significant cathodic shift of the reduction wave of poly(**8**) and a broadening of its oxidation feature above scan rates of 25 mV/s (Figure 9, bottom). Distortions at low scan rates are consistent with a lower degree of ion mobility for poly(**8**), particularly when compared with poly(**3**)−poly(**7**).

Electrochromic Studies. It is well established that electrochemical oxidation of polythiophene-type systems increases the degree of planarity along the main chain. As a result, an absorption feature typically appears near 700 nm and has been assigned to polaron-induced $\pi \rightarrow \pi^*$ transitions that occur along the backbone of the polymer.[23] Further oxidation of these materials gives rise to new absorption features in the NIR region that have been attributed to $\pi \rightarrow \pi^*$ bipolaron excitations.[48] In the case of the polymers described herein, metal-ligated imi-

(46) Tennyson, A. G.; Rosen, E. L.; Collins, M. S.; Lynch, V. M.; Bielawski, C. W. *Inorg. Chem.* **2009**, *48*, 6924–6933.
(47) Deng, Y.; Liu, S. J.; Fan, Q. L.; Fang, C.; Zhu, R.; Pu, K. Y.; Yuwen, L. H.; Wang, L. H.; Huang, W. *Synth. Met.* **2007**, *157*, 813–822.

Scheme 5. Proposed Mechanism of Polaron and Bipolaron Formation For Thin Films Poly(**4**)−Poly(**8**) in $TBAPF_6/CH_2Cl_2$ Solution under Oxidative Conditions

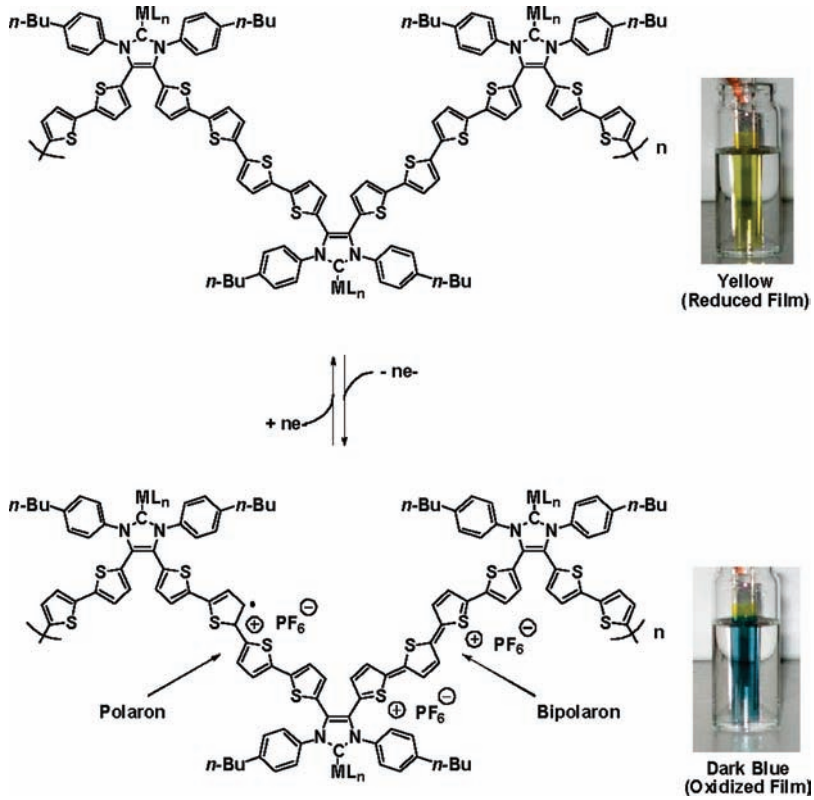

dazolylidene moieties are infused into the main chain and connected through quarterthiophene linkages. It was envisioned that polaron and bipolaron excitations would likewise occur at the oligothiophene linkages of poly(**4**)−poly(**8**); hence, these polymers were subsequently analyzed for their abilities to exhibit electrochromic characteristics.

Spectroelectrochemical measurements were performed on poly(**4**)−poly(**8**) by increasing the potential from 0.0 to 1.5 V in 0.1 V increments and in conjunction with the acquisition of UV−vis−NIR spectral data. An absorption feature near 700 nm was observed upon oxidation of a thin film of poly(**4**), which was found to be stable for 35 cycles. The material underwent a drastic color change from yellow (reduced state) to dark blue (oxidized state) during the oxidation process. Although similar results were obtained for poly(**5**) (Figure 10), this material was found to be stable for only 12 cycles, which is in accord with the labile nature of **5** in solution (vide supra). To underscore the importance of a coordinated transition metal, a thin film of poly(**6**) was also examined and found to exhibit diminished electrochromic behavior in comparison with thin films of poly(**4**) and poly(**5**). This observation suggested to us that the absorption features observed near 700 nm were enhanced by the presence of the coordinated transition metal.

On the basis of the data presented, combined with the well-known electrochromic properties of oligothiophenes, a proposed mechanism for the observed electrochromic activity is illustrated in Scheme 5. At high potentials, the quarterthiophene moieties undergo oxidation to generate polarons which causes the thiophenes to planarize. In turn, this results in the appearance of the new absorbances near 700 nm.[49] Since no significant NIR activity was observed, it is unlikely that bipolarons are being formed in the aforementioned materials. Nevertheless, in all cases studied, the polaron absorbance near 700 nm shifted hypsochromically above potentials of 1.2−1.3 V, which is likely due to overoxidation (with concomitant disruption of planarity along the main chain).[50]

Poly(**7**), which contains a coordinated iridium metal, exhibited a weak UV−vis absorption near 700 nm under oxidative conditions. In contrast, a thin film of poly(**8**) exhibited significant absorption at 692 and 1092 nm at 1.2 V (see Figure 11). The absorbance at 1092 nm was assigned to the formation of bipolarons along the quarterthiophene chains of poly(**8**) (see Scheme 5). In this respect, poly(**8**) is unique in that its CO ligands may facilitate the formation of polarons and bipolarons

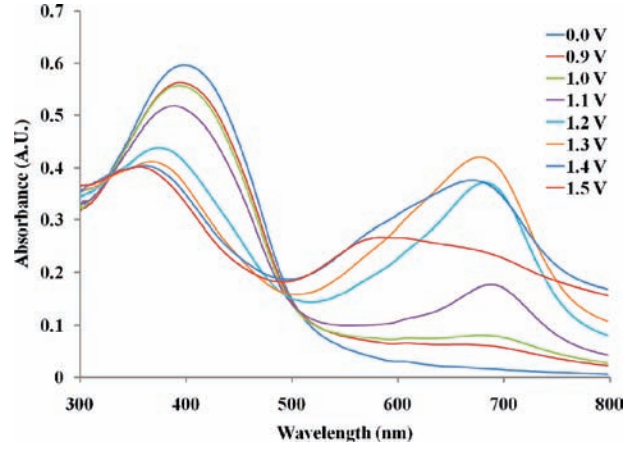

Figure 10. UV−vis profiles for silver NHC thin film poly(**5**) at different potentials (see color coded legend). The film was used as the working electrode of a three-electrode cell assembled in a quartz cuvette.

(48) For a recent review see: Beaujuge, P. M.; Reynolds, J. R. *Chem. Rev.* **2010**, *110*, 268–320.

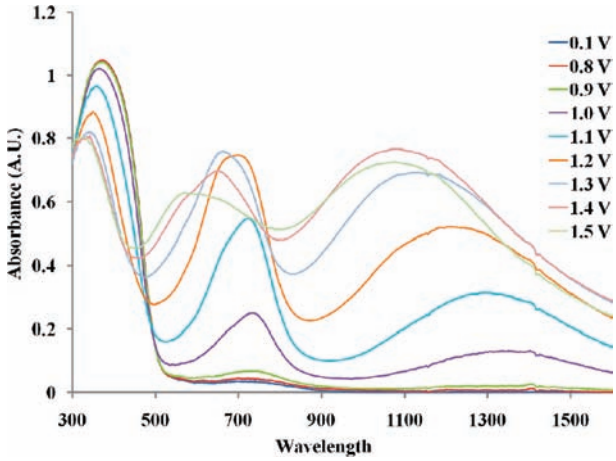

Figure 11. UV−vis−NIR profiles for iridium NHC thin film poly(**8**) at different potentials. The film was used as the working electrode of a three-electrode cell assembled in a quartz cuvette.

through the stabilization of these species (Figure 11). Regardless, thin films of poly(**8**) were found to be relatively robust as evidenced by the high degree of electrochromic reversibility observed (>50 cycles).

Conclusions

In summary, high-yielding syntheses of various silver, gold, iridium, and sulfur-substituted NHCs with bis(bithiophene) moieties have been synthesized and studied. Many of these complexes were successfully polymerized under oxidative conditions to afford stable thin films, which were characterized using a range of electrochemical, XPS, and UV−vis−NIR spectroscopic techniques and found to be consistent with their canonical structures. A unique feature of these materials is that the ligated main group or transition metals are orthogonally positioned with respect to the polymer main chain. In addition, most of the new polymers prepared were found to exhibit electrochromic characteristics that were dependent on the incorporated metal. Collectively, the results presented herein substantiate the pivotal role that NHCs and their ligated transition metals play in optimizing and enhancing the electronic properties exhibited by NHC-based polymeric materials.

Acknowledgment. We are grateful to the Robert A. Welch Foundation (Grant Nos. F-0003 and F-1621) for support of this work. We also thank Dr. Vince Lynch, Brent Norris, and Maria Cabezas for their assistance and the National Science Foundation (Grant No. 0618242) for the X-ray photoelectron spectrometer used in this work.

Supporting Information Available: ^{1}H and ^{13}C NMR, electrochemical studies of the Kuhn thione, diimine **1**, imidazolium chloride **2**, XPS, UV−vis, spectroelectrochemistry, and X-ray crystallographic data. This material is available free of charge via the Internet at http://pubs.acs.org.

JA104051X

(49) (a) Skotheim, T. A.; Reynolds, J. R. *Handbook of Conducting Polymers*; 3rd ed.; CRC Press: Boca Raton, 2007. (b) Farchioni, R.; Grosso, G. *Organic Electric Materials*; Springer-Verlag: Berlin, 2001.

(50) Tehrani, P.; Robinson, N. D.; Kugler, T.; Romonen, T.; Hennerdal, L. O.; Häll, J.; Malström, A.; Leenders, L.; Berggren, M. *Smart Mater. Struct.* **2005**, *14*, N21–N25.